Colloid and Polymer Science (2020) 298:637–651
https://doi.org/10.1007/s00396-020-04642-3

ORIGINAL CONTRIBUTION

Synthesis and characterization of low molar mass end-functionalized homo- and copolymers with ureidopyrimidone, UPy groups

Spyridoula-Lida Bitsi[1] · Maria Stogiou[1] · Salvatore Costanzo[2,3] · Emmanuel Stiakakis[4] · Dimitris Vlassopoulos[2,3] · Anastasia Nika[1,5] · Margarita Chatzichristidi[1,5] · Marinos Pitsikalis[1]

Received: 20 November 2019 / Revised: 21 February 2020 / Accepted: 13 March 2020 / Published online: 22 April 2020

Abstract

Anionic polymerization techniques along with functional initiation and/or functional termination reactions were employed for the synthesis of end-functionalized polymers composed from polystyrene (PS), polyisoprene-1,4 (PI), and polybutadiene-1,4 (PBd) chains bearing –OH end groups. Specifically, PS-OH, HO-PS-OH homopolymers, PS-*b*-PI-OH and PI-*b*-PS-OH block copolymers, HO-PS-*b*-PI-*b*-PS-OH triblock copolymers, and PS(PBd-OH)$_2$ miktoarm star copolymers were prepared. The –OH functions were transformed into 2–ureido–4–pyrimidone, UPy, groups leading to the synthesis of the corresponding functionalized polymers. The UPy groups interact through the formation of strong hydrogen bonds. The aggregation behavior of selected samples was studied by a variety of techniques, such as size exclusion chromatography, dilute solution viscometry, dynamic light scattering, differential scanning calorimetry, thermogravimetric analysis, melt rheology, small angle X-ray scattering, and atomic force microscopy. It was found that in the solid state and in non-polar solvents, the UPy-terminated chains associate leading to the formation of dimers and larger aggregates. This systematic study presents a library of useful materials for potential applications and for fundamental studies linking associations, molecular structure, and macroscopic properties.

Keywords Anionic polymerization · Hydrogen bonding · 2–ureido–4–pyrimidone · End-functionalized polymers · Aggregation

Introduction

Supramolecular chemistry based on non-covalent interactions has witnessed a tremendous progress over the last decades [1]. This scientific field was inspired by nature, since these kinds of interactions constitute the basis of biology and biochemistry [2, 3]. Vital operations with tremendous importance for the preservation of life, like molecular transportation, conformation of proteins, and the evolution of genetic information, are due to the presence of non-covalent bonds. In recent years, there is a continuous effort to employ the features of supramolecular chemistry in non-biological systems, as well [4–6]. Non-covalent bonds, especially multiple hydrogen bonding [7–26], metal-ligand complexes [27–35], ionic interactions, and van der Waals forces, have been widely used in molecular design, due to the ability of forming new supramolecular structures that exhibit thermoreversible characteristics. Dynamic systems [36–38] can be obtained through these non-covalent interactions. The association constants of these groups depend on the temperature, the solvent, and the solution concentration.

In their pioneering work, Meijer et al. [39–41] introduced 2–ureido–4–pyrimidone (UPy) as a structural unit for the formation of supramolecular polymers. This group has a unique hydrogen bonding sequence, a donor-donor-acceptor-acceptor (DDAA) arrangement, which is suitable for self-

Electronic supplementary material The online version of this article (https://doi.org/10.1007/s00396-020-04642-3) contains supplementary material, which is available to authorized users.

✉ Marinos Pitsikalis
pitsikalis@chem.uoa.gr

[1] Industrial Chemistry Laboratory, Department of Chemistry, National and Kapodistrian University of Athens, 15771 Panepistimiopolis Zografou, Athens, Greece

[2] Foundation of Research and Technology, Institute of Electronic Structure and Laser, Heraklion, 70013 Crete, Greece

[3] Department of Materials Science & Technology, University of Crete, Heraklion, 70013 Crete, Greece

[4] Institute of Complex Systems 3, Forschungszentrum Jülich, 52425 Jülich, Germany

[5] Department of Microelectronics, Institute of Advanced Materials, Physicochemical Processes, Nanotechnology and Microsystems, NCSR Demokritos, Athens, Greece

complementary interactions, leading to a rapid dimerization of the UPy groups via a strong quadruple hydrogen bond array in common organic solvents as well as in the melt. With an association constant of $K_{assoc} = 6 \times 10^7 M^{-1}$ in chloroform and $K_{assoc} = 6 \times 10^8 M^{-1}$ in toluene and a facile and quantitative synthesis involving a one-step procedure, UPy is an appropriate moiety for the preparation of supramolecular structures via molecular recognition.

New horizons have emerged in materials science through the combination of supramolecular and polymer chemistry. The incorporation of functional groups, which form noncovalent bonds, to polymeric chains leads to materials with novel properties and numerous practical applications, such as self-healing polymers, shape-memory polymers, and reversible gels [42–46]. The role of the UPy group in the enhancement of the physical properties of polymers has been established through the years by many research groups. Long et al. [47–49] have studied several functionalized macromolecules. UPy and other functional groups have been attached to polystyrene, PS, polyisoprene, PI, polystyrene-*b*-polyisoprene, PS-*b*-PI, and to other polymeric chains. Rheological and thermal studies led to the conclusion that reversible aggregates are formed in the bulk due to hydrogen bonding and are stable up to 80 °C. Viscometry studies, conducted on polyacrylates containing 10 mol% UPy groups, revealed that strong aggregates were formed only in non-polar solvents, such as toluene and chloroform. In polar solvents, supramolecular structures were not produced. The size and the stability of these aggregates depend on the number of UPy units at each macromolecular chain and the solution concentration [50, 51]. Recently, Baskaran et al. reported the synthesis of semi- and telechelic polybutadienes with UPy end groups and studied the association behavior of these homopolymers in non-polar solvents [52, 53]. The presence of aggregates through the interaction of the hydrogen forming UPy groups was verified by a variety of experimental techniques, both in solution and in the solid state.

Despite the important developments outlines above, a number of formidable challenges remain in this fascinating film. They relate to the quest to obtain a link between molecular structure and final properties, and in this respect a systematic investigation of the role of polymeric molar mass, type and structure of polymer, and position of functional groups are important. In this study, we report the synthesis and characterization of well-defined end-functionalized polymers having –OH end groups and composed from polystyrene (PS), polyisoprene-1,4 (PI), and polybutadiene-1,4 (PBd) chains. PS-OH, HO-PS-OH homopolymers, PS-*b*-PI-OH and PI-*b*-PS-OH block copolymers, HO-PS-*b*-PI-*b*-PS-OH triblock copolymers, and PS(PBd-OH)$_2$ miktoarm star copolymers were prepared by anionic polymerization techniques. The –OH functions were transformed to the corresponding UPy functions. The low molecular weight samples were employed to study the association behavior of the UPy-terminated polymers, both in solution and in the bulk. Compared with the samples of Long et al. [47–49], the PS homopolymers have much lower molecular weights, less than 1000, in the range of oligomers. In addition, the PS-*b*-PI block copolymers have much lower molecular weights as well (in the range of 1000 to 5000, compared with 8000 up to 59,000 in the previous study [47–49]). Furthermore, Long et al. [47–49] prepared diblocks bearing the functional groups only at the PI chain end, whereas in the present study the same groups were located at either the PS or PI chain end, as already mentioned. The association behavior was studied using a variety of experimental techniques, such as size exclusion chromatography (SEC), dilute solution viscometry, dynamic light scattering (DLS), differential scanning calorimetry (DSC), thermogravimetric analysis (TGA), melt rheology, small angle X-ray scattering (SAXS), and atomic force microscopy (AFM). The specific goals of this work are (i) to establish experimental techniques for the synthesis of UPy-functionalized complex macromolecular architectures; (ii) to follow the hierarchy of structures that are formed in solution and in the melt, starting from the dimerization through the formation of hydrogen bonds between the UPy groups up to the formation of higher aggregates, due to the association of the polar UPy groups in non-polar solvents and in the melt; and (iii) to identify the conditions under which aggregation is suppressed and only the dimerization of the UPy groups is present. A deeper understanding on the association behavior of these systems is provided in this work. In the near future, the effect of the macromolecular architecture on this aggregation process will be explored using either UPy moieties or other heterocomplementary groups forming hydrogen bonds.

Experimental section

Materials

All materials used to carry out the described experimental work were obtained from Sigma-Aldrich. The purification of the solvents, the monomers, the linking agents, and the additives was conducted according to the standards required by anionic polymerization high vacuum techniques, as reported in the literature [54–57]. The synthesis of the anionic initiator *sec*-BuLi was performed via the reaction of *sec*-BuCl with Li metal. The functional anionic initiator 3-(t-butyldimethylsilyloxy)-1-propyllitium (*t*BDMSPLi) was purchased from Lithium Corp. and used as received. Toluene and $CHCl_3$, used for the characterization experiments, were dried over CaH_2 and molecular sieves, respectively, and were distilled just prior to use.

Polymer synthesis

Conventional anionic polymerization high vacuum techniques were employed for the synthesis of the semitelechelic homopolymers and block copolymers PS-OH, PS-*b*-PI-OH, and PI-*b*-PS-OH, following literature procedures [58–61]. In all cases, the living polymers were terminated with ethylene oxide in order to introduce the end OH– group, followed by the addition of degassed methanol. The block copolymers were synthesized with sequential addition of the monomers. In the case of the PI-*b*-PS-OH sample, a small amount of tetrahydrofuran (THF) was added prior the addition of styrene. The telechelic polymer HO-PS-OH was obtained by a combination of the functional initiator *t*BDMSPLi, which was employed for the polymerization of styrene and termination of the living polymer with ethylene oxide. A two-fold excess of tetramethylene ethylene diamine (TMEDA) was employed to accelerate the initiation reaction [62]. The triblock copolymer HO-PS-*b*-PI-*b*-PS-OH was synthesized by employing the functional initiator, preparing the *t*-butyldimethylsilyloxy functionalized diblock PS-*b*-PI having half the molecular weight of the PI chains followed by linking the living chains with dichlorodimethylsilane. An excess of the living chains was employed followed, after the linking reaction, by fractionation in a system of good solvent/non-solvent (toluene/methanol) to remove the excess arm, using standard procedures of anionic polymerization and purification techniques. The deprotection of the –OH group was conducted by reacting the polymer with HCl in 10 fold excess over the *t*-butyldimethylsilyloxy groups in 1,4-dioxane, under reflux for 3 h. The miktoarm star PS(PBd-OH)$_2$ was prepared following literature procedures used for the synthesis of the corresponding PS(PBd)$_2$ stars [63–65]. The only difference is that the functional initiator *t*BDMSPLi was employed for the synthesis of the PBd arms and that after the purification of the final miktoarm star, the deprotection procedure was applied, as previously mentioned, to afford the desired product. The low molecular weight polymers were extensively purified by repeated extractions with distilled water to remove inorganic salts. The organic phase was dried over anhydrous $MgSO_4$ and filtered and the polymers were obtained by evaporation of the solvent in a rotary evaporator. Finally, the samples were dried in a vacuum oven.

Synthesis of 2-ureido-4-pyrimidone

1,6-Hexyl-diisocyanate (0.63 mol, 101 ml) was added under argon atmosphere to 2-amino-4-hydroxy-6-methylpyridine (0.90 mmol, 11 g). The reaction mixture was stirred for 16 h at 100 °C under reflux. Afterwards, the mixture was left to reach room temperature. Hexane was added to the solution and finally filtered through a Buchner filter. The product of the reaction was washed with hexane for three consecutive times and was left to dry at 50 °C under reduced pressure for 1 week to remove the excess of 1.6-hexyl-diisocyanate (yield 90%).

End-functionalization reaction with UPy

The hydroxyl-functionalized copolymers were transformed into the corresponding UPy-terminated samples using literature procedures [41]. Here, we discuss for example the introduction of the UPy group at the end of the PS-OH with M_n = 840 (g/mol), noting that similar procedures were adopted for all other samples. PS-OH (3.57 mmol, 3 g) was dissolved in dry $CHCl_3$ (120 ml), followed by the addition of UPy (7.14 mmol, 2.1 g), in a two-fold excess over the polymer and dibutyltin dilaurate (DBDTL) under argon atmosphere. The mixture was stirred at 60 °C for 16 h under reflux. Then, it was allowed to reach room temperature and after that it was filtered using a Buchner filter. A solution of the product in dry $CHCl_3$ (200 ml) with silica (2 g) and catalytic amount of DBDTL was reacted under the same conditions mentioned in previous reactions, in order to remove the excess of UPy. The pure product was filtered first and then precipitated into excess of methanol. Finally, the sample was dried at 50 °C under reduced pressure.

Characterization

Size exclusion chromatography (SEC) experiments were conducted at 40 °C using a modular instrument consisting of a Waters Model 510 pump, a Waters Model U6K sample injector, a Waters Model 401 differential refractometer, a Waters Model 486 UV spectrophotometer, and a set of 4-μ-Styragel columns with a continuous porosity range from 10^5 to 500 Å. The columns were housed in an oven thermostatted at 40 °C. THF was the carrier solvent at a flow rate of 1 ml/min. Experiments were also run in $CHCl_3$ at room temperature and at the same flow rate.

Dynamic light scattering (DLS) measurements were conducted with an ALV/CGS-3 compact 209 goniometer system, equipped with an ALV 5000/EPP multi-τ digital 210 correlator with 288 channels and an ALV/LSE-5003 light scattering electronics unit 211 for stepper motor drive and limit switch control. A JDS Uniphase 22-mW He-Ne laser 212 (λ = 632.8 nm) was used as the light source. The time autocorrelation function $g_2(q,t)$ of the scattering intensity I(q,t) was calculated according to [66]:

$$g_2(q,t) = < I(q,t)\, I(q,t+t_o) > / < I(t) >^2 \quad (1)$$

where t is the time, t_0 is the lag time, the <> operator denotes the average value, and q is the scattering wave vector:

$$q = 4\pi n_o \sin(\theta/2)/\lambda \quad (2)$$

with θ the scattering wave vector, the scattering (or observation) angle between the incident light and the scattered light (angle of observation), n_0 the optical index of the suspending medium, and λ the wavelength of the incident light. Measurements were carried out five times for each concentration and angle and were averaged. The solutions were filtered through 0.45-μm hydrophobic PTFE filters (Millex-LCR from Millipore) before measurements. The angular range for the measurements was 30–150°. The experimental correlation functions were analyzed by the cumulants method and the CONTIN software [67]. Typically, the decay of the autocorrelation function is well captured by an exponential decay, whose characteristic time depends on the diffusion coefficient of the scattering unit and yield a characteristic hydrodynamic size through the so-called Stokes-Einstein-Sutherland equation. When different scattering populations exist in the sample, the analysis of the scattering signal reveals a distribution of relaxation times which reflects different sizes.

Viscometric data were analyzed using the Huggins equation [68]:

$$\frac{\eta_{sp}}{c} = [\eta] + K_H[\eta]^2 c + \quad (3)$$

and the Kraemer equation [68]:

$$\frac{\ln \eta_r}{c}[\eta] + K_K[\eta]^2 c + \quad (4)$$

where η_r, η_{sp}, and $[\eta]$ are the relative, specific, and intrinsic viscosities, respectively, whereas K_H and K_K are the Huggins and Kraemer constants, respectively. All measurements were carried out at 25 °C. Cannon-Ubbelohde dilution viscometers equipped with a Schott-Geräte AVS 410 automatic flow timer were used.

^{1}H-NMR spectra were recorded in *d*-chloroform at 25 °C with a Varian Unity Plus 300/54 NMR spectrometer.

Differential scanning calorimetry (DSC) experiments were performed with a 2910 Modulated DSC model from TA instruments. The samples were heated or cooled at a rate of 10 °C/min.

Thermogravimetric analysis (TGA) experiments were conducted with a Q50 model from TA instruments. The heating rate was adjusted at 10 °C/min.

Rheological measurements were performed with an Antoon Paar MCR702 rheometer operating in the strain-control mode and equipped with a stainless-steel 8-mm parallel plate geometry. The temperature control was provided by a hybrid convection-peltier unit (CTD180) which can span a temperature range from − 10 to 180 °C. In order to prevent degradation of the samples, the rheological measurements were carried out in N_2 atmosphere. The samples having a glass transition temperature below room temperature are liquid-like at ambient conditions. These samples were loaded directly onto the rheometer by using a spatula. The other samples with a glass transition at about room temperature were shaped to 8-mm discs before loading, by using a hot press and a vacuum mold. The samples were annealed for 2 min at a temperature of 30 °C. The force applied to the mold was 0.5 ton. The sample quantity loaded into the mold was between 20 and 30 mg so that the discs had a thickness of approximately 0.5–0.6 mm. Since some of the samples have a long equilibration time, a vacuum oven was used to perform a pre-annealing before loading the samples in the rheometer.

In-house laboratory small angle X-ray scattering (SAXS) measurements were carried out at the high brilliance Galium Anode Low Angle X-ray Instrument (GALAXI) of the Jülich Center for Neutron Science (JCNS, Germany) [69]. A Dectris-Pilatus 1M detector with resolution of 981 × 1043 pixels and a pixel size of 172 × 172 μm was employed to record the 2D SAXS scattering patterns. The 2D SAXS patterns were integrated using FIT2D software. One-dimensional SAXS (1D-SAXS) profiles, at 20 °C for linear unentangled PS samples, carrying either the OH– or the UPy– end group, are shown in the figures below.

Atomic force microscopy (AFM) measurements were performed with a NT-MDT NTEGRA, equipped with an etalon tip with a resonance frequency of approximately 300 kHz and a force constant of about 30 N/m, in a semicontact mode.

Results and discussion

Polymer synthesis and characterization

Anionic polymerization is a well-known living polymerization technique leading to polymers with narrow molecular weight distributions and predicted molecular weights [58–61]. It also allows the synthesis of complex macromolecular architectures and functionalized polymers in a very well-controlled way [70–76]. The introduction of the end hydroxyl groups was accomplished by the reaction of the living polymers with ethylene oxide. It is a very well-established method for the quantitative introduction of the desired end OH– groups. The synthesis of the block copolymers was conducted with the sequential addition of monomers. In the case of the PI-*b*-PS-OH block copolymers, there is a need to have the living end at the PS chain end. Therefore, isoprene has to be polymerized first. In order to accelerate the crossover reaction from the polyisoprenyl lithium to the corresponding styryl lithium anions, a small amount of the polar THF was added prior the addition of styrene, using standard protocols of anionic polymerization. Under these conditions, well-defined polymers with narrow molecular weight distribution were obtained, as was revealed by SEC and NMR measurements. The molecular characteristics are summarized in Table 1. To appreciate the low molar masses in this table, note that the entanglement molar mass (corresponding for the formation of

Table 1 Molecular characteristics of the end-functionalized polymers

Sample	[a]M_n	[a]Đ	[b]%mole PS	%mol 1,4 PI or PBd
PS-OH#1	840	1.10	100	0
PS-OH#2	560	1.08	100	0
PS-OH#3	1300	1.13	100	0
PS-OH#4	8000	1.03	100	0
PS-OH#5	14,400	1.02	100	0
HO-PS-OH	6500	1.06	100	0
PS-*b*-PI-OH#1	1810	1.15	34.2	72.1
PS-*b*-PI-OH#2	950	1.15	39.6	67.5
PS-*b*-PI-OH#3	7000	1.03	53.1	90.1
PI-*b*-PS-OH#1	4780	1.10	35.1	89.6
PI-*b*-PS-OH#2	1870	1.17	37.4	89.2
PI-*b*-PS-OH#3	12,000	1.07	56.3	90.2
HO-PS-*b*-PI-*b*-PS-OH	25,000	1.04	60.0	90.4
$PS(PBd\text{-}OH)_2$	28,600	1.06	41.4	88.3

[a] By SEC in THF at 40 °C

[b] By ^{1}H-NMR in $CDCl_3$ at 25 °C

physical network) for PS is about 17,000 g/mol and for PI (1,4-addition) about 4500 g/mol [77].

The synthesis of the telechelic polystyrene HO-PS-OH was accomplished by using *t*BDMSPLi as a functional initiator. In order to break down the association of the organolithium species and thus accelerate the initiation reaction, the polar compound TMEDA was added in two-fold excess over the initiator. The living polymer was terminated by ethylene oxide, as mentioned previously (Scheme 1). A well-defined sample of low polydispersity was finally obtained. The protective *t*-butyldimethylsilyl group was removed by treatment with HCl in 1,4-dioxane, under reflux for 3 h. The success of the deprotection reaction was confirmed by ^{1}H NMR, through the disappearance of the characteristic *t*butyl silyl groups. An example is given in Figure S1 of the Supporting Information (SI).

The synthesis of the triblock copolymer HO-PS-*b*-PI-*b*-PS-OH was achieved by using the functional initiator in order to prepare the *t*-butyldimethylsilyloxy functionalized diblock PS-*b*-PI having half the molecular weight of the PI chains, followed by linking the living chains with dichlorodimethyl silane (Scheme 2). For the synthesis of the initial diblock copolymer, THF was used to accelerate the initiation reaction, since TMEDA is known to react with the chlorosilane. For the linking reaction, an excess of the living diblock was used in order to assure the synthesis of the desired product. This excess was finally removed by fractionation using toluene/methanol as the solvent/non-solvent system. The procedure was monitored by SEC, as shown in Figure S2. Deprotection of the protective group leads to the synthesis of the desired product.

The miktoarm star copolymer $PS(PBd\text{-}OH)_2$ was synthesized following the chlorosilane methodology and the approach adopted for the synthesis of AB_2 miktoarm stars, as shown in Scheme 3 [63–65]. Living PSLi was initially linked to a large excess of CH_3SiCl_3, followed by the evaporation of the excess silane. A small excess of the living polybutadienyllithium arm, prepared using the functional initiator, was finally linked to the macromolecular linking agent $PS(CH_3)SiCl_2$, leading to the synthesis of the desired product. The excess polydiene arm was removed by fractionation using a mixture of hexane/toluene 40/60 v/v as solvent and methanol as non-solvent. The reaction sequence was monitored by SEC, as shown in Figure S3. The deprotection reaction was conducted in acidic environment, yielding a miktoarm star bearing one PS arm and two PBd-OH arms, end-functionalized with OH– groups.

The introduction of the UPy end group to the prepared polymers was monitored by NMR analysis, as shown in Figure S4 for sample PS-UPy#1. The molecular weight calculated from the comparison of the integrals of the UPy proton signals with those of the aromatic protons of the main PS chain of the low molecular weight polymers is in very close agreement with the SEC data and the stoichiometric values, thus confirming the quantitative incorporation of the functional UPy groups at the end of the polymer chains. SEC analysis

Scheme 1 Synthesis of α,ω-telechelic homopolymers HO-PS-OH

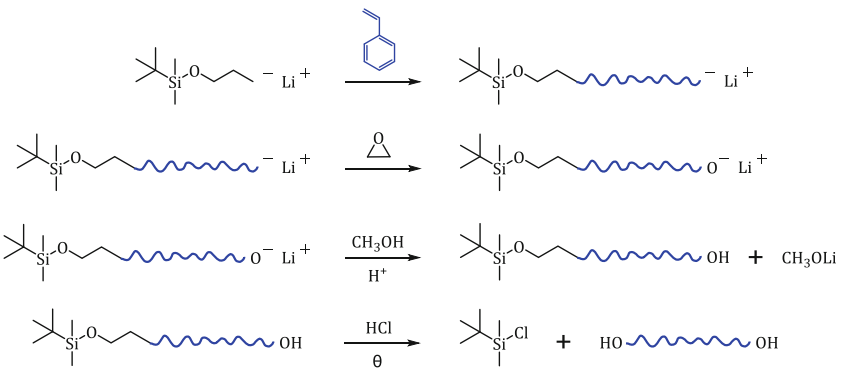

Scheme 2 Synthesis of α,ω-telechelic triblock copolymers HO-PS-b-PI-b-PS-OH

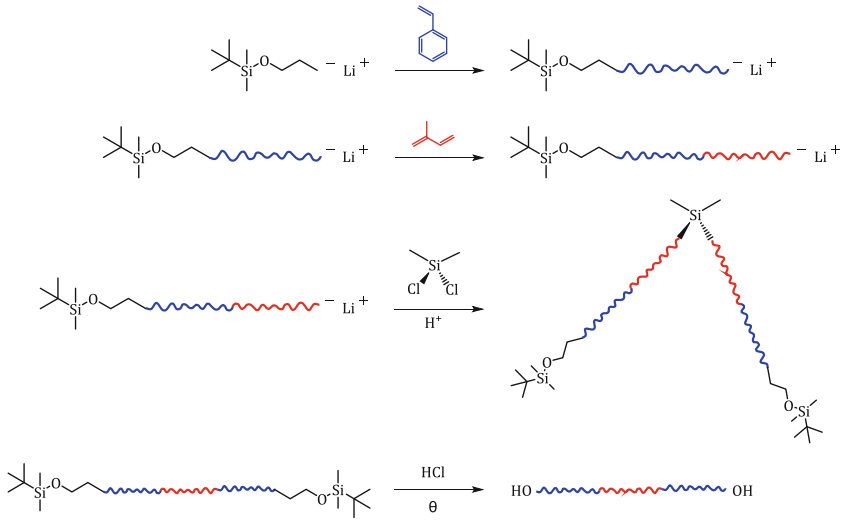

in THF prior and after the introduction of the UPy group showed the same traces without any signal of polymer degradation or crosslinking after the functionalization reaction, complying with earlier results in the literature [7–26]. Finally, a variety of end-functionalized polymers with molecular and structural homogeneity were prepared.

Solution properties: aggregation phenomena in low molecular weight polymers

SEC analysis in $CHCl_3$ It is very well established in the literature that the UPy groups can dimerize through the formation of a strong quadruple hydrogen bond array in common non-polar organic solvents. The association constant is as high as $K_{assoc} = 6 \times 10^7 M^{-1}$ in chloroform. In order to confirm this behavior and to further analyze the dilute solution and bulk properties of the polymers, due to the presence of the UPy groups, PS homopolymers and PS-*b*-PI block copolymers of low molecular weights were studied by a variety of techniques. In these polymers, the effect of the UPy group is expected to be much more pronounced; hence, it will be easier to trace it. The polymers with the OH– and with the UPy end groups were analyzed by SEC in $CHCl_3$ as the carrier solvent. There are no previous results in the literature from SEC

Scheme 3 Synthesis of telechelic miktoarm star copolymer $PS(PBd\text{-}OH)_2$

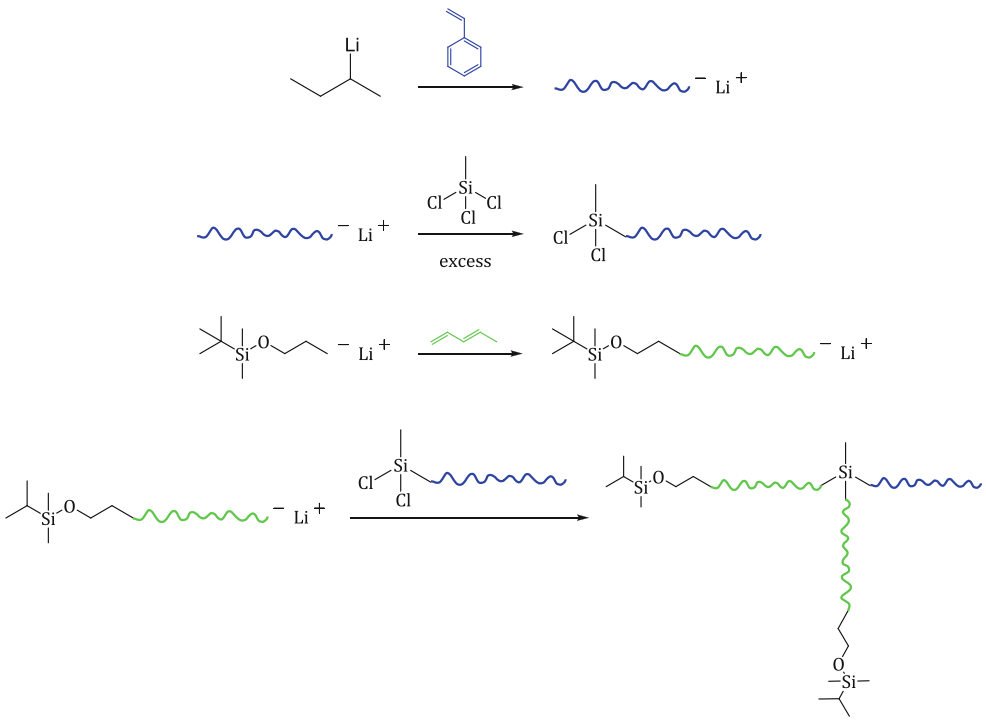

analysis on these low molecular weight end-functionalized polymers. Characteristic traces are given in Fig. 1, whereas more results are provided in Table S1 of the SI.

It is obvious that the traces of the UPy-functionalized polymers are moved to higher molecular weights or lower elution volumes. Their molecular weight is almost double compared with the corresponding –OH functionalized precursors. This is a direct evidence of dimerization of the UPy groups in $CHCl_3$ solutions. Except of the main peak, there are small shoulders or tails at higher and at lower molecular weights in all cases. These results may be tentatively as follows: There is a strong interaction between the UPy groups, leading to dimerization of the polymer chains. However, higher aggregates are also formed due to the interaction of the polar UPy groups, but they cannot survive the strong (shear/extensional) forces developed in the SEC columns. Therefore, only a small shoulder at higher molecular weights indicates the presence of these higher aggregates, whereas on the other hand, the small tail at lower molecular weights indicates the presence of single chains. In other words, there is a hierarchy of association in solution. The dimers are strong enough to survive the presence of external forces in SEC; however, most of the higher aggregates are disrupted under the same conditions. Note on the other hand, the dimers are dissociated to a small extend leading to the formation of free chains. Finally, only small traces at both higher and lower elution volumes appear at the SEC trace. This speculative picture will be further confirmed by the results of other characterization methods (especially DLS) below. Therefore, a dynamic equilibrium is established in the solution, which is sensitive to the application of external forces. The diblock copolymers PI-*b*-PS-UPy, bearing the functional group at the end of the PS block, show reduced tendency of dimerization, suggesting that the dimers are not

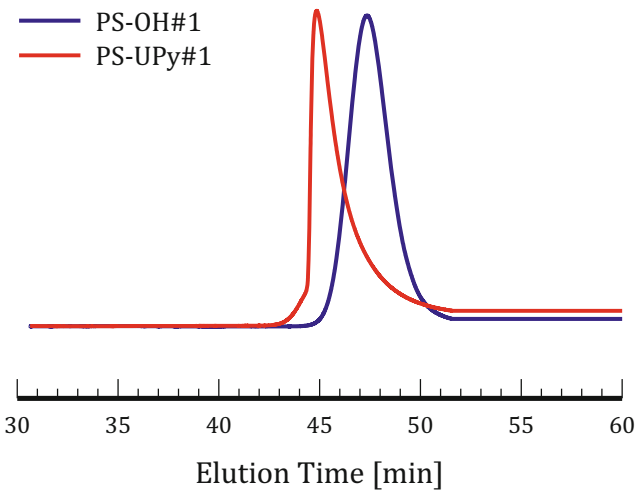

Fig. 1 SEC traces of the functionalized polymer PS-UPy#1 and its precursor PS-OH#1 in $CHCl_3$ at 25 °C

so strong as in the other homo- and copolymer cases. This may be the result of the higher molecular weight of these samples and the attachment of the UPy group to the less flexible block, which prevents the formation of stronger associates.

Dilute solution viscometry Measurements were conducted in toluene, a non-polar solvent which is able to promote the interaction of the functional end groups. Both the –OH and the –UPy-functionalized polymers were investigated. The results are provided in the SI (Table S2, Figure S5). The intrinsic viscosities of the –OH functionalized polymers are low enough and comparable with the corresponding non-functionalized samples. The results are in close agreement with those reported in the literature for low molecular weight PS in toluene at 25 °C [78, 79]. This is a direct evidence that the –OH groups are not polar enough to promote association in this solvent, even for those very low molecular weight chains. This is in agreement with the SEC data, where no evidence of association was observed for the –OH functionalized polymers as well. However, it is clear that the Huggins constants for these samples are very high. This can be attributed on the one hand to the very low molecular weights of the chains and on the other hand to a weak interaction of the –OH groups. Still, this interaction is not strong enough to promote significant association and formation of stable aggregates.

A different situation is observed with the –UPy-functionalized samples. Both the intrinsic viscosity values and the Huggins constants are much higher compared with their –OH precursors. This is a direct indication of the presence of associates in solution. The shear forces applied in the capillary tube are not strong enough to break down the association. This is not unexpected since the viscometer is designed to obtain the zero-shear viscosity in dilute solution. The intrinsic viscosities of PS-*b*-PI-UPy are higher than that of PI-*b*-PS-UPy copolymers, meaning that the degree of association is higher in the former case, in agreement with SEC data. Finally, it is clear that in all cases both the Huggins and Kraemer plots show linear dependence on concentration over the examined range, implying that the associates are stable under the experimental conditions employed for the dilute solution viscosity measurements.

Dynamic light scattering DLS measurements were conducted in toluene at different concentrations, temperatures, and scattering angles, θ. Detailed measurements were conducted for the PS-UPy homopolymers in toluene. The data for PS-UPy#1 at $\theta = 90^{o}$ and different temperatures indicate that extended association exists. There are unimers, dimers but mainly higher-order associates in equilibrium, as inferred by the distribution of relaxation times obtained from CONTIN analysis (Figure S6). Upon heating from room temperature to 55 °C, the unimers and the dimers remain unchanged in the

solution, whereas the number of populations is gradually decreased and the larger aggregates tend to disappear (Figure S6). These results indicate that most of the polymer chains are aggregated into weak clusters which upon heating break-up into smaller structures. Subsequent cooling fails to yield the same association picture in solution, suggesting that this procedure is not reversible, at least at the same timeframe. It seems that the system needs more time to self-organize into dimers and larger clusters. Therefore, the kinetics of the association process is also important for the evaluation of the behavior of these end-functionalized polymers.

The dependence of the DLS data (distribution of relaxation times and mode intensities, as revealed by the CONTIN analysis) on the scattering angle suggests that the aggregates, especially the larger ones, are not spherical, as reported in the literature (Figure S7) [80–82]. More elongated structures seem to exist in the solution. Similar results were obtained from DLS measurements in linear PBds bearing UPy end groups in toluene [52]. Different populations exist in solution with extended clusters and both the angular and temperature dependence are very pronounced. Therefore, this behavior is attributed to the UPy end groups and not to the polymer chains, since toluene is a good solvent for both the linear PS and PBd. Further systematic analysis of DLS data at different concentrations will be conducted in the future.

Melt properties

Thermal analysis The thermal properties of the synthesized polymers were studied by means of DSC and TGA. The DSC measurements for the homo- and the block copolymers are summarized in Table 2, whereas characteristic thermograms are provided in the SI (Figure S8).

The Tg values of the PS homopolymers bearing the –OH end groups are very low, as expected for these very low molecular weight samples. These results are in agreement with other experimental results and theoretical predictions in the literature taking into account differences regarding the polymer end groups, the molecular weight distributions, the rates of sample heating/cooling, and the method of measuring of the Tg of the samples [83–87]. However, the corresponding values for the UPy-terminated chains are much higher. This is attributed to the presence of the end group interactions through the formation of hydrogen bonds. These interactions are very strong between the UPy units and reduce the mobility of the functionalized block segments. This effect is dramatically enhanced by the relatively low molecular weight of the chains, which promotes a significant contribution of the end group. Viscometry and, more importantly, DLS revealed the presence of strong aggregation of samples bearing UPy end groups in solution. This behavior is even more pronounced in the melt state, as indicated by the substantial increase of the Tg values of the UPy-functionalized polymers. This effect has been previously reported for linear homopolymers and block copolymers having the same functional end groups [47–52, 78, 79].

Table 2 DSC results of the end-functionalized polymers

Sample	M_n	Đ	Tg		
PS-OH#1	840	1.10	8.4		
PS-Upy#1			42.6		
PS-OH#2	560	1.08	0.1		
PS-Upy#2			20.9		
PS-OH#3	1300	1.13	31.2		
PS-Upy#3			51.2		
PS-OH#4	8000	1.03	65.6		
PS-Upy#4			77.5		
PS-OH#5	14,400	1.02	72.4		
PS-Upy#5			81.7		
HO-PS-OH	6500	1.06	72.4		
Upy-PS-Upy			81.9		
PS-*b*-PI-OH#1	1810	1.15	− 26.2		
PS-*b*-PI-Upy#1			− 16.8		
PS-*b*-PI-OH#2	950	1.15	− 29.7		
PS-*b*-PI-Upy#2			− 19.4		
PI-*b*-PS-OH#1	4780	1.10	− 53.1		
PI-*b*-PS-Upy#1			− 35.0		
PI-*b*-PS-OH#2	1870	1.17	− 46.5		
PI-*b*-PS-Upy#2			− 18.7		
PI-*b*-PS-OH#3	12,000	1.07	50.2	− 54.3	
PI-*b*-PS-Upy#3			64.5	− 47.2	
HO-PS-*b*-PI-*b*-PS-OH	25,000	1.04	− 49.5	53.0	87.6
Upy-PS-*b*-PI-*b*-PS-Upy			− 45.9	44.8	88.8
$PS(PBd\text{-}OH)_2$	28,600	1.06	− 87.7	71.7	
$PS(PBd\text{-}Upy)_2$			− 83.6	74.7	

The very low molecular weight block copolymers exhibit only one Tg value, suggesting that there is a mixing between the two phases. This single Tg value was substantially increased upon switching from the OH– to the –UPy group, due to the stronger hydrogen bonding interactions and the strong association of the latter. In the past, PS-*b*-PI blocks of higher molecular weights were synthesized bearing similar end groups. It was found that the Tg of the block not carrying the functional group hardly changed compared with the unfunctionalized copolymer. However, the Tg of the other block with the functional group increased appreciably. The effect was much more pronounced for the UPy-terminated samples, compared with the hydroxyl-functionalized copolymers [88]. In the case of the higher molecular weight copolymer PI-b-PS-OH#3, a partial mixing of the two phases was obtained, as inferred from the closeness of the two different Tg values compared with the respective homopolymers. Replacing the OH– group by the corresponding –UPy group,

the Tg of the PS phase was more influenced than that of the PI phase, in agreement with previous observations [88]. Finally, for the highest molecular weight samples, the effect of the end groups in Tg was negligible.

Table S3 of the SI provides the TGA data of UPy– and the –OH functionalized polymers, whereas example plots of the thermal decomposition are given in Figure S9. Comparing the decomposition patterns of these two polymers, it is evident that in the latter case, there is a first decomposition step at lower temperatures (less than 300 °C), which is attributed to the thermal decomposition of the functional UPy group, in agreement with previous studies [88]. The second decomposition step is more or less similar for the block copolymers and is attributed to the thermal degradation of the low molecular weight copolymers. More pronounced differences were obtained between the –OH and the UPy-functionalized PS homopolymers. In addition, more complex decomposition patterns were observed. These effects can be attributed to the stronger association of the very low molecular weight chains.

X-ray scattering Figure 2 depicts the one-dimensional SAXS profiles of linear unentangled PS carrying either the –OH (PS-OH#1, PS-OH#2) or the UPy (PS-UPy#1, PS-UPy#2) end group, at 20 °C. Since the UPy end group has a unique hydrogen bonding DDAA sequence, it acts as a monovalent attractive site and no branching is expected for PS-UPy#1,#2 samples. Therefore, only dimer aggregates should be formed, which can further associate into larger clusters and consequently, network formation is not possible, as will be confirmed rheologically below. Note also that the presence of a narrow q_s peak in the scattering patterns of PS-UPy melts and the unambiguous increase of its intensity with increasing the PS molecular weight (from PS-UPy#2 to PS-UPy#1) could be attributed to polymer chains aggregation driven by the polar nature of the UPy– end group. However, this effect is expected to be more pronounced by decreasing the molecular weight of PS; both the SAXS and rheological data (discussed below) indicate the opposite trend. Also this unusual effect is supported from the AFM image of UPy#3 with even higher MW (see Fig. 6 below). Since the samples have been properly equilibrated, we speculate that this is a consequence of the different aggregation in the two case. However, the two (small) molecular weights do not differ significantly (about 30%); hence, more work with additional molecular weights will be needed in the future to fully address this issue.

Samples PS-UPy#1,2 and PS-OH#1,2 were pre-annealed at 60 °C for 24 h. For sample PS-UPy#1,2, thermal scanning SAXS experiments between 5 and 60 °C did not show any temperature dependence of the scattering peaks, both upon cooling and heating (Fig. 2). This suggests that there is no indication of phase transition in this temperature range, which is also evident from the successful temperature superposition on the rheological data of Fig. 5 below, as well as the DLS measurements reported above. In Fig. 2c, d, the narrow and broad peaks, which are marked as q_S and q_B, respectively, have no clear structural origin; however, we note that they are virtually temperature-independent for all samples.

Melt rheology Further, we examine the linear viscoelastic response of linear unentangled PS melts carrying either the –OH or the –UPy end group. As taken from the vials, these telechelic samples were out of equilibrium state. In fact, the loss and storage moduli evolved with time indicating that the supramolecular structures were not fully developed. For this

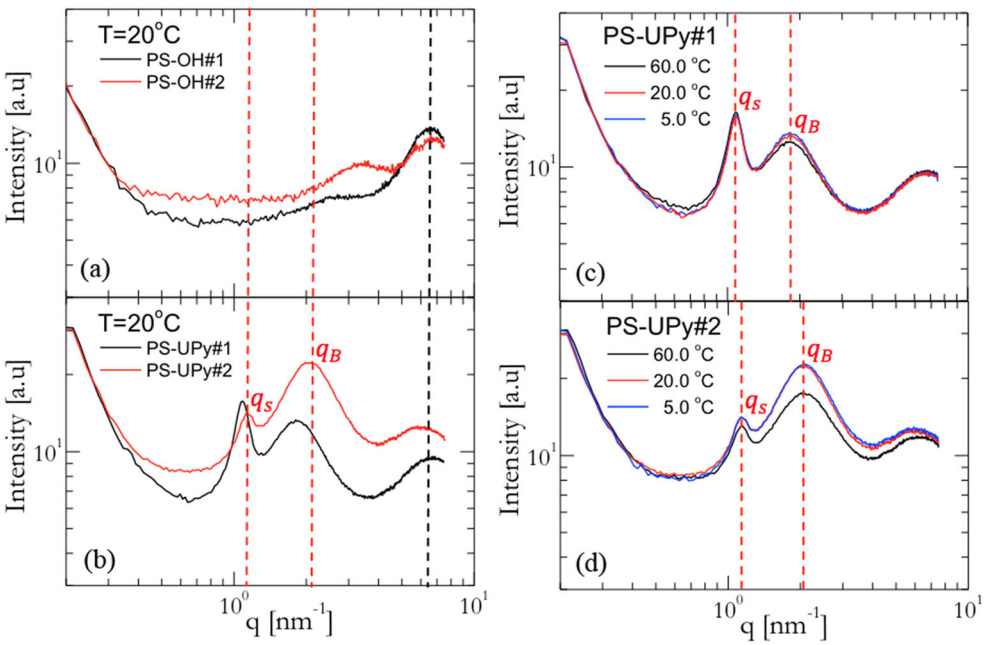

Fig. 2 SAXS profiles at 20 °C for linear unentangled PS melts carrying either (a) OH– end group or (b) UPy– end group. The black dashed line is a guide for the molecular weight dependence of the high q correlation peak. (c, d) Temperature-dependent SAXS profiles of the (c) PS-UPy#1 and (d) PS-UPy#2. The red dashed lines are a guide for the temperature dependence of the sharp (q_S) and broad (q_B) correlation peaks

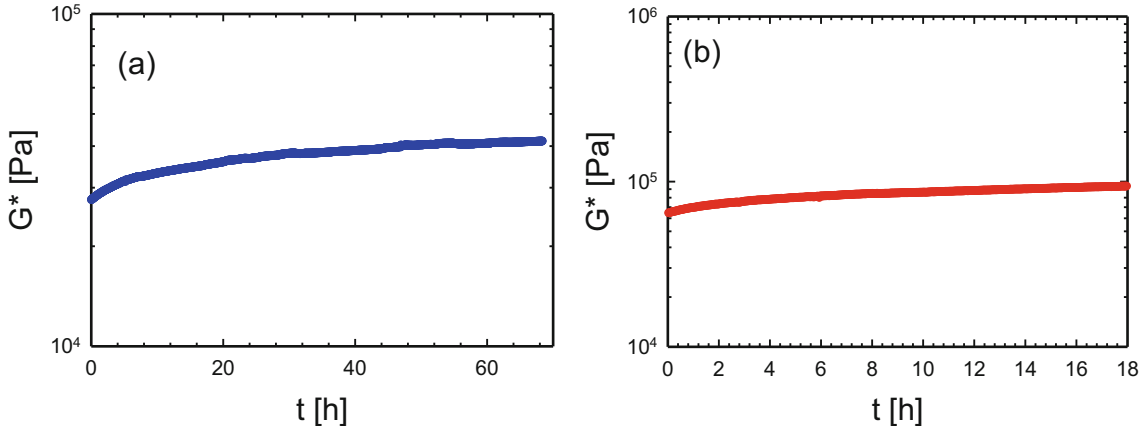

Fig. 3 (a) Equilibration of the sample PS-OH#2 at T = 50 °C and (b) equilibration of the sample PS-UPy#2 at T = 50 °C. In (b), the sample was pre-annealed for 10 days in vacuum oven at the same temperature

reason, the samples were first loaded into the rheometer and a dynamic time sweep test was performed in the linear regime until the moduli reached a steady (equilibrium) value. Figure 3a depicts the time evolution of the complex modulus G* of PS-OH#2 at 50 °C, which represents its equilibration process. Despite the fact that the sample is above its Tg (see Table 2), its equilibration took about 80 h, during which the moduli increased before attaining a plateau. Based on these results, the equilibration process was not followed for each sample, but instead the materials were pre-conditioned by annealing in a vacuum oven as mentioned above. This procedure helped in reducing the equilibration time, as reported in Fig. 3b, which shows the equilibration of PS-UPy#2 at 50 °C following pre-annealing for 10 days at 50 °C.

After equilibration, the linear dynamic response of the samples was measured at different temperatures and master curves were made according to the time-temperature superposition principle (TTS). We note that, due to hydrogen bonding, the TTS principle works only in an apparent way here. However, a fair superposition was found between the frequency responses of each sample at different temperatures, and this allowed to assemble the master curves of the viscoelastic moduli (see supporting info, figure S10). The samples exhibited viscoelastic liquid behavior, with G′>G″ over the whole frequency range measured. For this reason, the dynamic response is reported as complex viscosity vs frequency in Fig. 4 at the same distance from Tg (Tref = Tg + 40 °C). The complex viscosity of the sample PS-OH2 was lower than the sample PS-OH1, as expected. In fact, the molecular weight of PS-OH1 is almost double with respect to the molecular weight of PS-OH2. However, if we extract the zero-shear viscosities of both samples, the increase of viscosity induced by the substitution of the –OH group with the –UPy group is much larger than the expected scaling of log(η) vs log(Mw) in the

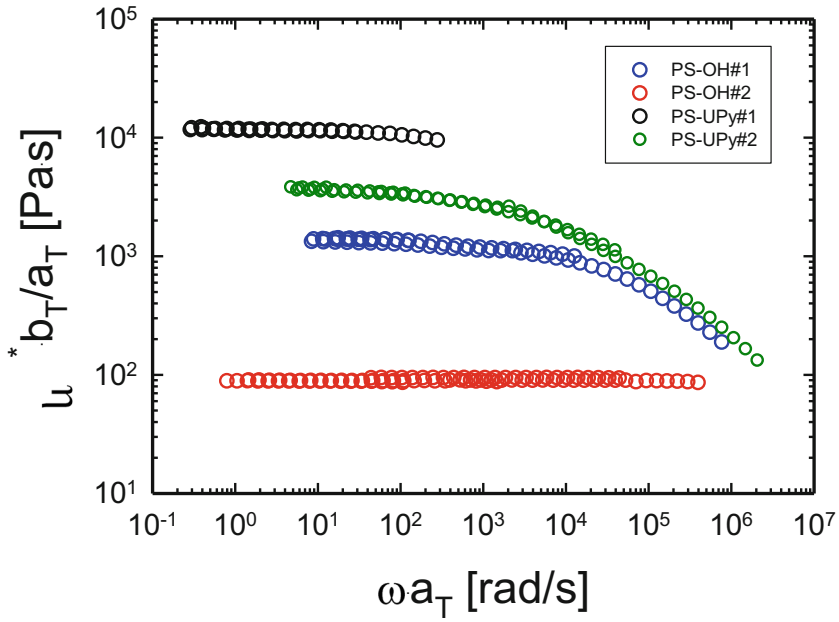

Fig. 4 Complex viscosity master curves of the samples at $T_{ref} = T_g + 40$ °C

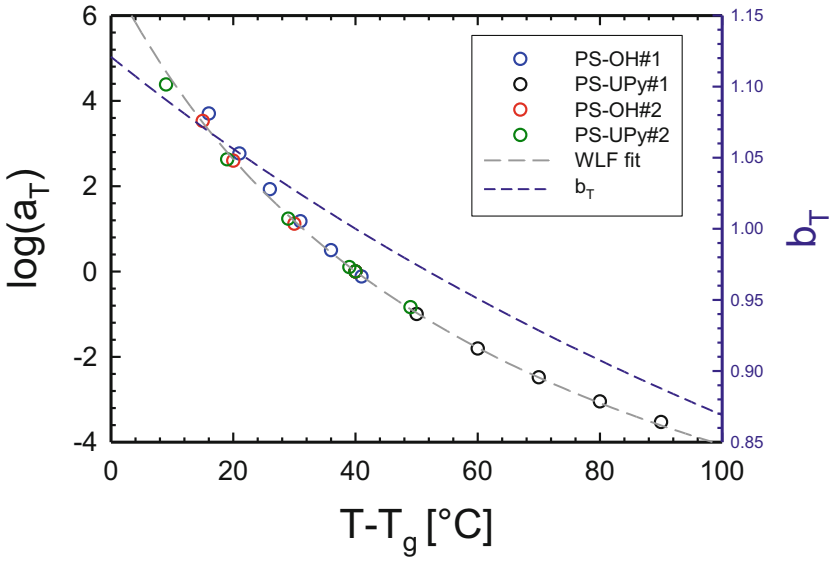

Fig. 5 Shift factors of PS-OH#1, PS-OH#2, and PS-UPy#2 compared at the same distance from the glass transition. c_1 = 9.73, c_2 = 65.51 °C

unentangled regime. This indicates that the presence of strongly hydrogen bonding groups, such as UPy, induces the formation of transient ordered structures which yield a strong increase in the viscosity. The viscosity of PS-UPy1 is larger than that of PS-UPy2 as expected. In fact, the Mw of PS-UPy1 is almost double than that of PS-UPy2.

The shift factors used to manually build the master curves of Fig. 4 are reported in Fig. 5. The data at different temperature were first vertically shifted according to temperature/density compensation criterion. Hence, the vertical shift factor was calculated as $b_T = \rho_0 T_0/(\rho T)$. The temperature dependence of the density was taken as $\rho(T) = 1250–0.605$ T, with T expressed in °K (Zoller and Walsh). In example, Fig. 5 reports the vertical shift factor at the reference temperature of 40 °C. After vertical shifting, the data were manually shifted in order to achieve the best horizontal superposition. The horizontal shift factors were then fitted according to the William-Landel-Ferry equation, and reported at the same distance from Tg. Figure 5 reports the shift factors corresponding to the different samples as function of T-Tg. All data collapse on a single master curve. The average values of the constants are c_1 = 11.19 and c_2 = 105.2 °C. The WLF fit of the figure was calculated based on these values.

Atomic force microscopy Large-scale images of polymers with UPy end groups revealed the presence of fibrous-like structures, which are not continuous but are disrupted occasionally. Characteristic AFM images are shown in Fig. 6 and in Figure S12. These structures are composed of smaller spherical clusters arranged into cylindrical arrays. The presence of these elongated structures has been already verified by DLS measurements in dilute solution (see discussion above). These findings are in agreement with those obtained by Baskaran et al. with PBd-UPy polymers, having similar low molecular weight samples (M_n = 900–7700) [52]. The small clusters associating into elongated fibers are not well-defined and

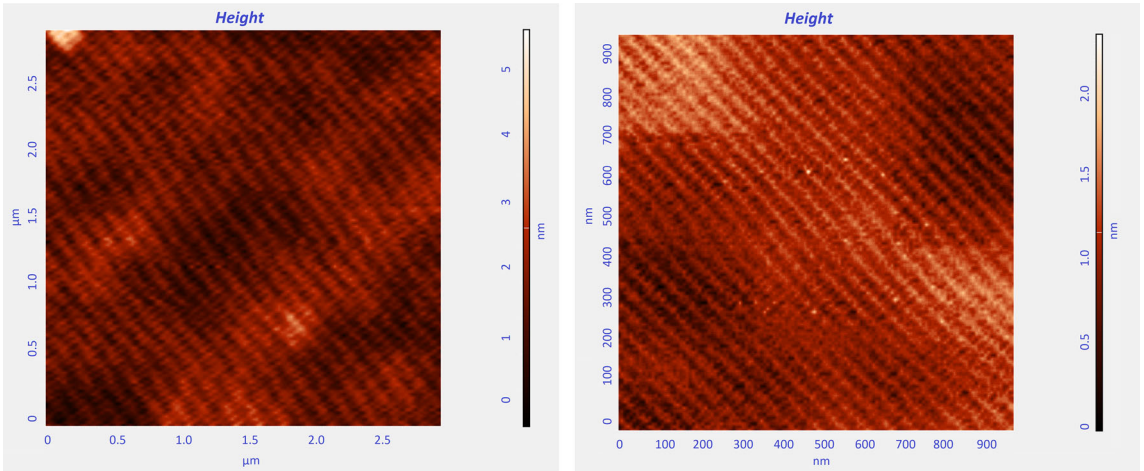

Fig. 6 AFM height images for sample PS-UPy#3: 3 μm (left) and 1 μm (right)

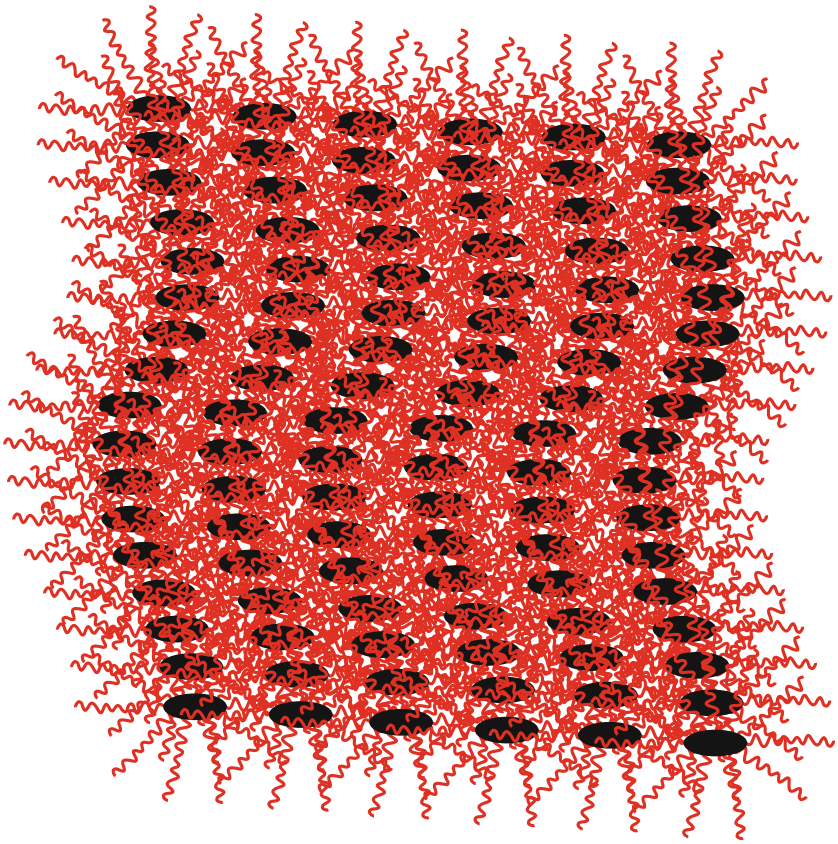

Scheme 4 Graphical representation of the PS-UPy#3 aggregates

therefore their sizes could not be determined unambiguously. However, the elongated structures are of the order of several nm and have no preferred direction, forming a macroscopic network. These structures are stable due to the absence of any force of field, but upon heating or applying shear forces (for example in the capillary viscosimeter), they seem to break into smaller clusters. The effect is more pronounced in the case of the block copolymers, due to the higher molecular weights of the samples (see Table 2). These results support the emerging picture from the SAXS and melt rheology measurements. Therefore, a hierarchy of structures is achieved: The UPy moieties originally form dimers, due to the formation of hydrogen bonds and then are further organized to more or less spherical clusters in non-polar solvents and in the melt. These clusters are finally arranged in cylindrical arrays, as shown schematically in Scheme 4.

Conclusions

A series of end-functionalized polymers composed of polystyrene, polyisoprene, and polybutadiene chains bearing –OH end groups were obtained by high vacuum anionic polymerization techniques. Specifically, well-defined PS-OH, HO-PS-OH homopolymers, PS-*b*-PI-OH and PI-*b*-PS-OH block copolymers, HO-PS-*b*-PI-*b*-PS-OH triblock copolymers, and $PS(PBd\text{-}OH)_2$ miktoarm star copolymers were prepared. The –OH functions were transformed to the hydrogen bond forming UPy groups, leading to the synthesis of the corresponding functionalized polymers. The low molecular weight polymers bearing the UPy groups strongly associated both in solution and in bulk. SEC in $CHCl_3$ revealed the formation of dimers through the formation of hydrogen bonds. Higher aggregates were unstable due to the application of strong forces in the SEC columns. Dilute solution viscometry in a capillary tube confirmed the formation of higher aggregates due to both the increased intrinsic viscosity and Huggins constants values. In that case, the weak shear forces applied in the capillary tube were not able to disrupt the association between the chains. DLS data indicated the equilibrium between single chains, dimers, and higher aggregates in non-polar solvents. These non-spherical were sensitive to changes in temperature. Selective data from AFM, SAXS, and melt rheology confirmed the presence of aggregates, their organization, and dynamics. DSC and TGA also supported the presence of extended association in the solid state. Hence, a hierarchy of structures was obtained starting from dimers, then to spherical aggregates and finally to cylindrical arrays.

Funding information The present work was co-funded by the European Union (ESF, Marie Sklodowska-Curie ITN "Supolen," grant no. 607937 and Horizon2020-INFRAIA-2016 EUSMI, grant no.731019) and Greek national funds through the Operational Program "Human Resources

Development, Education and Lifelong Learning," project title "Macromolecular architecture via hydrogen bonds. Synthesis, Characterization, Properties" (project code: 5006393).

References

1. Lehn J–M (1995) Supramolecular chemistry: concepts and perspectives. VCH Weinheim. https://doi.org/10.1002/adma.19960081029
2. Dietrich B, Lehn J–M, Sauvage J–P (1969) Les Cryptates. Tetrahedron Lett 10:2889–2892. https://doi.org/10.1016/S0040-4039(01)88300-3
3. Dietrich B, Lehn J–M, Sauvage J–P, Blanzat J (1973) Cryptates—X: syntheses et proprietes physiques de systemes diaza-polyoxa-macrobicycliques. Tetrahedron 29:1629–1645. https://doi.org/10.1016/S0040-4020(01)83409-8
4. Dietrich B, Lehn J–M, Sauvage J–P (1973) Cryptates—XI: complexes macrobicycliques, formation, structure, proprieties. Tetrahedron 29:1647–1658. https://doi.org/10.1016/S0040-4020(01)83410-4
5. Pedersen CJ (1988) Die Entdeckung der Kronenether (Nobel-Vortrag). Angew Chem Int Ed Engl 100:1053–1059. https://doi.org/10.1002/ange.19881000805;
6. Cram DJ, Cram JM (1974) Host-guest chemistry: complexes between organic compounds simulate the substrate selectivity of enzymes. Science 183:803–809. https://doi.org/10.1126/science.183.4127.803
7. Sijbesma RP, Meijer EW (1999) Self-assembly of well-defined structures by hydrogen bonding. Curr Opin Coll Inter Sci 4:24–32. https://doi.org/10.1016/S1359-0294(99)00011-4
8. ten Cate AT, Sijbesma RP (2002) Coils, rods and rings in hydrogen-bonded supramolecular polymers. Macromol Rapid Commun 23:1094–1112. https://doi.org/10.1002/marc.200290011
9. Sijbesma RP, Meijer EW (2003) Quadruple hydrogen bonded systems. Chem Commun:5–16. https://doi.org/10.1039/B205873C
10. Beijer FH, Kooijiman H, Spek AL, Sijbesma RP, Meijer EW (1998) Self-complementarity achieved through quadruple hydrogen bonding. Angew Chem Int Ed Engl 37:75–78. https://doi.org/10.1002/(SICI)1521-3773(19980202)37:1/2<75::AID-ANIE75>3.0.CO;2-R
11. Jørgensen WL, Pranata J (1990) The importance of secondary interactions in triply hydrogen-bonded complexes: guanine-cytosine vs. uracil-diaminopyridine. J Am Chem Soc 112:2008–2010. https://doi.org/10.1021/ja00161a061
12. Brunsveld L, Folmer JB, Meijer EW, Sijbesma RP (2001) Supramolecular polymers. Chem Rev 101:4071–4097. https://doi.org/10.1021/cr990125q
13. Beijer FH, Sijbesma RP, Vekemans JAJM, Meijer EW, Kooijiman H, Spek AL (1996) Hydrogen-bonded complexes of diaminopyridines and diaminotriazines: opposite effect of acylation on complex stabilities. J Org Chem 61:6371–6380. https://doi.org/10.1021/jo960612v
14. Murray TJ, Zimmerman SC (1992) New triply hydrogen bonded complexes with highly variable stabilities. J Am Chem Soc 114:4010–4011. https://doi.org/10.1021/ja00036a079;
15. Hamilton AD, Van Engen D (1987) Induced fit in synthetic receptors: nucleotide base recognition by a molecular hinge. J Am Chem Soc 109:5035–5036. https://doi.org/10.1021/ja00250a052
16. Kyogoku Y, Lord RC, Rich A (1969) An infrared study of the hydrogen-bonding specificity of hypoxanthine and other nucleic acid derivatives. Biochim Biophys Acta 179:10–17. https://doi.org/10.1016/0005-2787(69)90116-6
17. Fenlon EE, Murray TJ, Baloga MH, Zimmerman SC (1993) Convenient synthesis of 2-amino-1,8-naphthyridines, building blocks for host-guest and self-assembling systems. J Org Chem 58:6625–6628. https://doi.org/10.1021/jo00076a021
18. Murray TJ, Zimmerman SC, Kolotuchin SV (1995) Synthesis of heterocyclic compounds containing three contiguous hydrogen bonding sites in all possible arrangements. Tetrahedron 51:635–648. https://doi.org/10.1016/0040-4020(94)00922-H
19. Zimmerman SC, Murray TJ (1995) 7-amido-1,8-naphthyridines as hydrogen bonding units for the complexation of guanine derivatives: the role of 2-alkoxyl groups in decreasing binding affinity. Tetrahedron Lett 36:7627–7630. https://doi.org/10.1016/0040-4039(95)01586-7
20. Schmuck C, Wienand W (2001) Self-complementary quadruple hydrogen-bonding motifs as a functional principle: from dimeric supramolecules to supramolecular polymers. Angew Chem Int Ed Engl 40:4363–4369. https://doi.org/10.1002/15213773(20011203)40:23<4363:AIDANIE4363>3.0.CO;2-8
21. Zeng H, Miller RS, Flowers RA, Gong B (2000) A highly stable, six-hydrogen-bonded molecular duplex. J Am Chem Soc 122:2635–2644. https://doi.org/10.1021/ja9942742
22. Folmer BJB, Sijbesma RP, Kooijiman H, Spek AL, Meijer EW (1999) Cooperative dynamics in duplexes of stacked hydrogen-bonded moieties. J Am Chem Soc 121:9001–9007. https://doi.org/10.1021/ja991409v
23. Yang X, Hua F, Yamato K, Ruckenstein E, Gong B, Kim W, Ryu CY (2004) Supramolecular AB diblock copolymers. Angew Chem Int Ed 43:6471–6474. https://doi.org/10.1002/anie.200460472
24. Kunz MJ, Hayn G, Saf R, Binder WH (2004) Hydrogen-bonded supramolecular poly(ether ketone)s. J Polym Sci Polym Chem Ed 42:661–674. https://doi.org/10.1002/pola.10858
25. Binder WH, Bernstorff S, Kluger C, Petraru L, Kunz MJ (2005) Tunable materials from hydrogen-bonded pseudo block copolymers. Adv Mater 17:2824–2828. https://doi.org/10.1002/adma.200501505
26. Binder WH, Kunz MJ, Ingolic E (2004) Supramolecular poly(ether ketone)–polyisobutylene pseudo-block copolymers. J Polym Sci Polym Chem Ed 42:162–172. https://doi.org/10.1002/pola.10979
27. Gohy J-C, Lohmeijer BGG, Schubert US (2003) From supramolecular block copolymers to advanced nano-objects. Chem Eur J 9:3472–3479. https://doi.org/10.1002/chem.200204640
28. Gohy J-C, Lohmeijer BGG, Alexeev A, Wang X-S, Manners I, Winnik MA, Schubert US (2004) Cylindrical micelles from the aqueous self-assembly of an amphiphilic poly(ethylene oxide)-b-poly(ferrocenylsilane) (PEO-b-PFS) block copolymer with a metallo-supramolecular linker at the block junction. Chem Eur J 10:4315–4323. https://doi.org/10.1002/chem.200400222
29. Gohy J-C, Lohmeijer BGG, Schubert US (2002) Metallo-supramolecular block copolymer micelles. Macromolecules 35:4560–4563. https://doi.org/10.1021/ma012042t
30. Gohy J-C, Lohmeijer BGG, Varshney SK, Schubert US (2002) Covalent vs metallo-supramolecular block copolymer micelles. Macromolecules 35:7427–7435. https://doi.org/10.1021/ma0204812
31. Gohy J-C, Lohmeijer BGG, Varshney SK, Décamps B, Leroy E, Boileau S, Schubert US (2002) Stimuli-responsive aqueous micelles from an ABC metallo-supramolecular triblock copolymer. Macromolecules 35:9748–9755. https://doi.org/10.1021/ma021175r
32. Gohy J-C, Lohmeijer BGG, Schubert US (2002) Reversible metallo-supramolecular block copolymer micelles containing a soft core. Macromol Rapid Commun 23:555–560. https://doi.org/10.1002/1521-3927(20020601)23:9<555::AID-MARC555>3.0.CO;2-K
33. Mayer G, Vogel V, Lohmeijer BGG, Gohy J-C, Van den Broek JA, Haase W, Schubert US, Schubert D (2004) Metallo-supramolecular

block copolymer micelles: improved preparation and characterization. J Polym Sci Polym Chem Ed 42:4458–4465. https://doi.org/10.1002/pola.20263
34. Gohy J-C, Lohmeijer BGG, Décamps B, Leroy E, Boileau S, Van den Broek JA, Schubert D, Haase W, Schubert US (2003) Synthesis and characterization of metallo-supramolecular micelles. Polym Int 52:1611–1618. https://doi.org/10.1002/pi.1348
35. Gohy J-C, Hofmeier H, Alexeev A, Schubert US (2003) Aqueous micelles from supramolecular graft copolymers. Macromol Chem Phys 204:1524–1530. https://doi.org/10.1002/macp.200350017
36. Sijbesma RP, Beijer FH, Brunsveld L, Folmer BJB, Hirschberg JHKK, Lange RFM, Lowe JKL, Meijer EW (1997) Reversible polymers formed from self-complementary monomers using quadruple hydrogen bonding. Science 278:1601–1604. https://doi.org/10.1126/science.278.5343.1601
37. Söntjens SHM, Sijbesma RP, van Genderen MHP, Meijer EW (2001) Selective formation of cyclic dimers in solutions of reversible supramolecular polymers. Macromolecules 34:3815–3818. https://doi.org/10.1021/ma002010q
38. Kelly JR, Maguire MP (1987) A receptor for the oriented binding of uric acid type molecules. J Am Chem Soc 109:6549–6551. https://doi.org/10.1021/ja00255a072
39. Söntjens SHM, Sijbesma RP, van Genderen MHP, Meijer EW (2000) Stability and lifetime of quadruply hydrogen bonded 2-ureido-4[1H]-pyrimidinone dimers. J Am Chem Soc 122:7487–7493. https://doi.org/10.1021/ja000435m
40. Beijer FH, Sijbesma RP, Kooijiman H, Spek AL, Meijer EW (1998) Strong dimerization of ureidopyrimidones via quadruple hydrogen bonding. J Am Chem Soc 120:6761–6769. https://doi.org/10.1021/ja974112a
41. Folmer BJB, Sijbesma RP, Versteegen RM, van der Rijt JAJ, Meijer EW (2000) Supramolecular polymer materials: chain extension of telechelic polymers using a reactive hydrogen-bonding synthon. Adv Mater 12:874–878. https://doi.org/10.1002/1521-4095(200006)12:12<874::AID-ADMA874>3.0.CO;2-C
42. Wojteki RJ, Nelson A (2016) Small changes with big effects: tuning polymer properties with supramolecular interactions. J Polym Sci Part A: Polym Chem Ed 54:457–472. https://doi.org/10.1002/pola.27940
43. Kumpfer JR, Rowan SJ (2011) Thermo-, photo-, and chemo-responsive shape-memory properties from photo-cross-linked metallo-supramolecular polymers. J Am Chem Soc 133:12866–12874. https://doi.org/10.1021/ja205332w
44. Li J, Viveros A, Wrue MH, Anthamatten M (2007) Shape-memory effects in polymer networks containing reversibly associating side-groups. Adv Mater 19:2851–2855. https://doi.org/10.1002/adma.200602260
45. Cordier P, Tournilhac F, Soulie-Ziakovic LL (2008) Self-healing and thermoreversible rubber from supramolecular assembly. Nature 451:977–980. https://doi.org/10.1038/nature06669
46. Vogt AP, Sumerlin BS (2009) Temperature and redox responsive hydrogels from ABA triblock copolymers prepared by RAFT polymerization. Soft Matter 5:2347–2351. https://doi.org/10.1039/B817586A
47. Yamauchi K, Lizotte JR, Long TE (2002) Synthesis and characterization of novel complementary multiple-hydrogen bonded (CMHB) macromolecules via a michael addition. Macromolecules 35:8745–8750. https://doi.org/10.1021/ma020961t
48. Yamauchi K, Lizotte JR, Long TE (2003) Thermoreversible poly(alkyl acrylates) consisting of self-complementary multiple hydrogen bonding. Macromolecules 36:1083–1088. https://doi.org/10.1021/ma0212801
49. Yamauchi K, Kanomata A, Inoue T, Long TE (2004) Thermoreversible polyesters consisting of multiple hydrogen bonding (MHB). Macromolecules. 37:3519–3522. https://doi.org/10.1021/ma049913u
50. Yamauchi K, Lizotte JR, Hercules DM, Vergne MJ, Long TE (2002) Combinations of microphase separation and terminal multiple hydrogen bonding in novel macromolecules. J Am Chem Soc 124:8599–8604. https://doi.org/10.1021/ja020123e
51. McKee MG, Elkins CL, Park T, Long TE (2005) Influence of random branching on multiple hydrogen bonding in poly(alkyl methacrylate)s. Macromolecules 38:6015–6023. https://doi.org/10.1021/ma050667b
52. Bobade S, Malmgren T, Baskaran D (2014) Micellar-cluster association of ureidopyrimidone functionalized monochelic polybutadiene. Polym Chem 5:910–920. https://doi.org/10.1039/C3PY01002C
53. Bobade S, Wang Y, Mays J, Baskaran D (2014) Synthesis and characterization of Ureidopyrimidone Telechelics by CuAAC "Click" reaction: effect of Tg and polarity. Macromolecules 47:5040–5050. https://doi.org/10.1021/ma5007705
54. Hadjichristidis N, Iatrou H, Pispas S, Pitsikalis M (2000) Anionic polymerization: high vacuum techniques. J Polym Sci Part A Polym Chem 38:3211–3234. https://doi.org/10.1002/1099-0518(20000915)38:18<3211::AID-POLA10>3.0.CO;2-L
55. Uhrig D, Mays JW (2005) Experimental techniques in high-vacuum anionic polymerization. J Polym Sci Part A Polym Chem 43:6179–6222. https://doi.org/10.1002/pola.21016
56. Hadjichristidis N, Hirao A Eds. Chapter 1 page 3, Ratkanthwar K, Zhao J, Zhang H, Hadjichristidis N, Mays J.W (2015) Anionic Polymerization. Principles, practice, strength, consequences and applications, Springer Japan
57. Hadjichristidis N, Hirao A, Eds chapter 2, page 19, Ratkanthwar K, Hadjichristidis N, Mays JW (2015) Anionic Polymerization. Principles, practice, strength, consequences and applications, Springer Japan
58. Hadjichristidis N, Pitsikalis M, Pispas S, Iatrou H (2001) Polymers with complex architecture by living anionic polymerization. Chem Rev 101:3747–3792. https://doi.org/10.1021/cr9901337
59. Hadjichristidis N, Hirao A (eds) (2015) Anionic Polymerization. Principles, practice, strength, consequences and applications. Springer, Japan
60. Morton M (1983) Anionic polymerization: principles and practice. Academic Press, New York
61. Bywater S (1979) Preparation and properties of star-branched polymers. Adv Polym Sci 30:89–116. https://doi.org/10.1007/3-540-09199-8_2
62. Patil AO, Schulz DN, Novak BM (1998) Functional Polymes. Modern synthetic methods and novel structures. ACS Symp. Ser. 704, chapter 5, Sutton, DE, and Schwindeman, JA page 58,
63. Hsieh HL, Quirk RP (1996) Anionic Polymerization. Principles and practical applications. Marcel Dekker, New York
64. Hadjichristidis N, Pitsikalis M, Iatrou H, Sakellariou G (2009) in Controlled and living polymerizations. From mechanisms to applications Müller, A.H.E., Matyjaszewski, K. Eds., Wiley VCH, chapter 7, 343
65. Hadjichristidis N, Pitsikalis M, Iatrou H, Driva P, Sakellariou G, Chatzichristidi M (2012) Polymers with star-related structures: Polym Sci: A Compreh Ref 6:29–111. https://doi.org/10.1016/B978-0-444-53349-4.00161-8
66. Berne BJ, Pecora R (1976) Dynamic light scattering. Academic Press
67. Provencher SW (1982) CONTIN: a general purpose constrained regularization program for inverting noisy linear algebraic and integral equations. Comput Phys Commun 27:229–242. https://doi.org/10.1016/0010-4655(82)90174-6
68. Sperling LH Introduction to physical polymer science, 4th Edition, Chapter 3, John Wiley & Sons Inc. Hoboken, New Jersey

69. Kentzinger E, Krutyeva M, Rücker U (2016) Jülich Centre for neutron science. GALAXI: Gallium anode low-angle x-ray instrument. Journal of Large-Scale Research Facilities, JLSRF 2(A61):1–5. https://doi.org/10.17815/jlsrf-2-109
70. Pitsikalis M, Pispas S, Mays JW, Hadjichristidis N (1998) Nonlinear block copolymer architectures. Adv Polym Sci 135:1–137. https://doi.org/10.1007/3-540-69191-X_1
71. Hadjichristidis N, Iatrou H, Pitsikalis M, Pispas S, Avgeropoulos A (2005) Linear and non-linear triblock terpolymers. Synthesis, self-assembly in selective solvents and in bulk. Progr Polym Sci 30:725–782. https://doi.org/10.1016/j.progpolymsci.2005.04.001
72. Hadjichristidis N, Iatrou H, Pitsikalis M, Mays JW (2006) Macromolecular architectures by living and controlled/living polymerizations. Progr Polym Sci 31:1068–1132. https://doi.org/10.1016/j.progpolymsci.2006.07.002
73. Patil AO, Schulz DN, Novak BM, Functional Polymes. Modern synthetic methods and novel structures (1998) ACS Symp Ser 704 Chapter 8, Hadjichristidis N, Pitsikalis M, Pispas S, page 96
74. Pitsikalis M, Hadjichristidis N (1995) Model mono-, di-, and tri-.omega.-functionalized three-arm star polybutadienes. Synthesis and association in dilute solutions by membrane osmometry and static light scattering. Macromolecules 28:3904–3910. https://doi.org/10.1021/ma00115a023
75. Pitsikalis M, Hadjichristidis N, Mays JW (1996) Model mono-, di-, and tri-ω-functionalized three-arm star polybutadienes. Association Behavior in Dilute Solution by Dynamic Light Scattering and Viscometry. Macromolecules 29:179–184. https://doi.org/10.1021/ma951001s
76. Hadjichristidis N, Pispas S, Pitsikalis M (1999) End-functionalized polymers with zwitterionic end-groups. Progr Polym Sci 24:875–915. https://doi.org/10.1016/S0079-6700(99)00018-0
77. Fetters LJ, Lohse DJ, Colby RH (2007) in Physical Properties of Polymers Handbook, J.E. Mark Editor, Springer, New York
78. Rossi C, Bianchi U, Bianchi E (1960) Diffusion and viscosity of low polymers in solution. J Polym Sci 41:31–39. https://doi.org/10.1002/macp.1960.020410104
79. Rossi C, Bianchi E (1959) Diffusion measurements on low molecular weight polystyrenes. J Polym Sci 41:189–197. https://doi.org/10.1002/pol.1959.1204113815
80. Burchard W (1996) In: Brown W (ed) Combined static and dynamic light scattering in light scattering. Principles and Development. Oxford University Press, Oxford, p 445
81. Schurtenberger P (1996) Light scattering in complex micellar systems in light scattering. Principles and development; Brown W Ed.; Oxford University Press: Oxford, U.K., p 296
82. Higgins J, Benoit HC (1996) Polymers and neutron scattering. Oxford University Press, Oxford, Chapter 7, p 241
83. Fox Jr TG, Flory PJ (1950) Second-order transition temperatures and related properties of polystyrene. I. Influence of molecular weight. J Appl Phys 21:580–591. https://doi.org/10.1063/1.1699711
84. Fox Jr TG, Flory PJ (1954) The glass temperature and related properties of polystyrene. Influence of molecular weight. J Polym Sci 49:315–319. https://doi.org/10.1002/pol.1954.120147514
85. Reding FP, Faucher JA, Whitman RD (1962) Glass transitions in ethylene copolymers and vinyl homopolymers and copolymers. J Polym Sci 57:483–498. https://doi.org/10.1002/pol.1962.1205716538
86. An L, He D, Jing J, Wang Z, Yu D, Jiang B (1997) Effects of molecular weight and interaction parameter on the glass transition temperature of polystyrene mixtures and its blends with polystyrene/poly (2,6-dimethyl-p-phenylene oxide). Eur Polym J 33:1523–1528. https://doi.org/10.1016/S0014-3057(97)00089-X
87. Claudy P, Létoffé JM, Camberlain Y, Pascault JP (1983) Glass transition of polystyrene versus molecular weight. Polym Bull 9:208–215. https://doi.org/10.1007/BF00283709
88. Karatzas A, Talelli M, Vasilakopoulos T, Pitsikalis M, Hadjichristidis N (2006) Micellization of ω-functionalized diblock copolymers in selective solvent. Study on the Effect of Hydrogen Bonds. Macromoleculess 39:8456–8466. https://doi.org/10.1021/ma061396n